processes

MDPI

Article

A Two-Stage Robust Capacity Optimal Configuration Model for Power Systems Considering Multi-Objective Optimization

Zhixiang Wang, Xirui Jiang *, Zheng Fan and Yanan Wu

National Key Laboratory of Advanced Power Transmission Technology, China Electric Power Research Institute, Beijing 102209, China; wangzx_epri@163.com (Z.W.); fanzheng@epri.sgcc.com.cn (Z.F.); wuyanan@epri.sgcc.com.cn (Y.W.)

* Correspondence: jiangxirui@epri.sgcc.com.cn

Abstract

To mitigate renewable energy curtailment and maintain long-term power balance, both planning and operational strategies must be addressed. However, most existing studies on power system capacity optimization focus on a single objective, such as economic efficiency or carbon reduction. To overcome this limitation, this paper proposes a two-stage robust capacity optimization and decision-making framework for power systems that incorporates multi-objective optimization. In the first stage, a bi-level robust capacity optimization model is developed, where the upper-level problem targets capacity expansion planning and the lower-level problem addresses chronological production simulation and operational optimization. The upper-level objectives include minimizing investment and operating costs, maximizing supply reliability, and maximizing renewable energy integration. Secondly, the NSGA-II algorithm is employed to solve the constructed bi-level multi-objective optimization model. Finally, a decision-making model based on the Best–Worst Method (BWM), entropy weighting, and the Technique for Order Preference by Similarity to Ideal Solution (TOPSIS) is constructed to further evaluate and select among multiple Pareto-optimal solutions obtained in the first stage, thereby determining the final capacity configuration scheme. The case study demonstrates that the proposed two-stage framework maintains good stability under scenarios such as extreme weather, ensuring a power supply reliability of 98.78% and a new energy utilization rate of 98.5% under various conditions.

Keywords: multi-objective optimization; chronological production simulation; capacity optimization; multi-attribute decision making

check for updates

Academic Editors: Yun Ii Go and Wolf-Gerrit Früh

Received: 10 September 2025
Revised: 15 October 2025
Accepted: 24 October 2025
Published: 4 November 2025

Citation: Wang, Z.; Jiang, X.; Fan, Z.; Wu, Y. A Two-Stage Robust Capacity Optimal Configuration Model for Power Systems Considering Multi-Objective Optimization. *Processes* **2025**, *13*, 3545. https://doi.org/10.3390/pr13113545

Copyright: © 2025 by the authors. Licensee MDPI, Basel, Switzerland. This article is an open access article distributed under the terms and conditions of the Creative Commons Attribution (CC BY) license (https://creativecommons.org/licenses/by/4.0/).

1. Introduction

1.1. Background and Motivation

In the context of increasingly severe environmental challenges such as global warming, the development of renewable energy has become a crucial approach to alleviating the contradiction between energy supply and demand [1]. Accelerating the construction of a new-type power system that accommodates the rising share of renewable energy is an essential pathway to achieving carbon peaking and carbon neutrality goals for the energy sector and society at large [2–4]. Accordingly, governments worldwide have successively proposed energy transition path and new power system development plans, bringing profound changes to the global energy landscape [5,6]. At the ninth meeting of the Central Financial and Economic Affairs Commission, President of China Xi Jinping first proposed

the establishment of a new-type power system. Subsequently, the National Development and Reform Commission (NDRC) and other governmental departments issued the Action Plan for Accelerating the Construction of a New-type Power System, marking the entry of China's new power system development into a critical phase of full-scale initiation and accelerated advancement [7,8]. By the end of 2024, China's installed wind power capacity had reached 520 GW, and photovoltaic capacity had reached 886 GW, both ranking first in the world.

With the large-scale development and high penetration of renewable energy, new challenges have emerged for maintaining long-term supply–demand balance and power supply reliability in power systems, leading to increasingly severe curtailment of wind and solar power [9,10]. The direct cause of this issue lies in the limited absorption capacity of the system, while the fundamental cause is the inherent volatility of renewable energy output and the insufficient flexibility of system regulation [11].

1.2. Literature Review and Research Gap

To reduce renewable energy curtailment and ensure long-term power balance, both system planning and operation must be addressed [12,13]. Among these, the effective power system planning is the primary concern [14]. Compared with traditional planning methods that mainly focus on short-term daily balance, it is now urgent to assess the risks of long-term supply–demand imbalances and to develop novel planning techniques that account for long-term balancing requirements in new-type power systems [15]. In addition, production simulation serves as a crucial tool for power system analysis, particularly in balancing studies, by optimizing the output of different generating units and other indicators to provide guidance for both operation and planning [16].

In terms of power system planning theory, numerous studies have focused on system planning under high renewable energy penetration, with optimization objectives including economic efficiency, carbon reduction [17], and multi-energy complementarity [18]. To adequately capture the characteristics of power system planning with high renewable energy integration, it is essential to account for renewable energy uncertainty. For example, Verastegui et al. [19] evaluated the flexibility requirements associated with short-term operational uncertainties in power systems and subsequently proposed an adaptive robust optimization model for generation and transmission expansion planning. Nunes et al. [20] considered both long-term and short-term uncertainties of highly variable renewable energy sources and developed a stochastic multi-stage planning model to optimize generation and transmission investments, thereby supporting alternative renewable energy policy targets. In addition, some scholars argue that power system planning should not be treated as a single-stage optimization problem but rather as a multi-stage coupled process. For instance, Li et al. [21] incorporated system variability and flexibility into a multi-stage generation expansion planning model.

Power system production simulation provides a basis for the planning and development of renewable energy [22]. Li et al. [23] argued that traditional planning methods lack chronological data on wind power and load demand, and proposed a non-sequential production simulation model to evaluate wind power curtailment. Qi et al. [24] employed chronological production simulation with a 15-min resolution to conduct fine-grained flexibility assessments of the power system, which then served as the basis for allocating flexibility resources. Yang et al. [25] performed operational simulations of power systems based on representative scenarios and used the results to support investment decisions in both battery storage and hydrogen storage. These studies indicate that production simulation, as a fundamental tool for assessing power balance, has become a central focus in contemporary power system planning.

In summary, existing power system planning theories are relatively well developed but are mainly oriented toward short-term intraday balancing and seldom account for multiple objectives such as supply reliability and renewable energy integration. To address these gaps, this study develops a bi-level robust capacity optimization model for power systems, where the upper-level problem focuses on capacity expansion planning and the lower-level problem addresses chronological production simulation and operational optimization. By further integrating a multi-scheme decision-making model, a two-stage decision-making framework for power system capacity optimization is established.

1.3. Contribution

The main contributions of this paper are as follows:

(1) Ensuring long-term power balance under multiple scenarios, including extreme weather conditions;

(2) Proposing a power system capacity optimization model that incorporates multiple objectives across economic, social, and environmental dimensions;

(3) Developing a decision-making model for capacity configuration schemes based on the Best–Worst Method (BWM), entropy weighting, and the Technique for Order Preference by Similarity to Ideal Solution (TOPSIS).

1.4. Paper Organization

The remainder of this paper is organized as follows. Section 2 introduces the proposed two-stage robust capacity optimization framework considering multiple objectives, including the multi-scenario generation method, the bi-level capacity optimization model, and the decision-making model for capacity configuration schemes. Section 3 presents a case study and multi-scenario analysis, and Section 4 concludes with key findings and recommendations.

2. Methodology

2.1. Bi-Level Optimization Model for Power System Capacity

2.1.1. Upper-Level of Long-Term Capacity Optimization Model

The objective of the upper-level model is to minimize the total installed capacity cost of different types of power sources within the region. The decision variables include the installed capacities of wind power, photovoltaic (PV), and other generation resources, as well as the transmission channel capacities.

Objective Function

(1) Objective 1: Minimization of installation and operational costs

The objective function for optimizing the capacities of multiple generation types and transmission channels in the new power system is to minimize the total cost. Specifically, it first accounts for the fundamental installation and operational costs of power sources. In addition, to ensure the regional integration and export of renewable energy, the function incorporates the construction cost of renewable energy grid connections, with particular emphasis on the expansion of transmission channels.

$$\min f_1 = (C^{\mathrm{Gen}} + C^{\mathrm{Trans}}) \tag{1}$$

where C^{Gen} represents the power installation cost; C^{Trans} represents the construction cost of the power transmission lines.

The total installation cost comprises the fixed costs associated with newly installed capacities and the operational costs of all power plants over the planning horizon. In

this model, the installed capacities of conventional thermal power, coal-fired units, and renewable energy sources are explicitly considered. The corresponding formulation is expressed as follows:

$$C^{\text{Gen}} = C^{\text{G}}_{\text{fix}} + C^{\text{G}}_{\text{run}} \tag{2}$$

$$C^{\text{G}}_{\text{fix}} = \begin{array}{c} P^{G,\text{new}}_{\text{coal}} * C_{\text{coal}} + P^{G,\text{new}}_{\text{hydro}} * C_{\text{hydro}} + {}^{G,\text{new}}_{\text{nuclear}} * C_{\text{nuclear}} \\ + {}^{G,\text{new}}_{\text{pv}} * C_{\text{pv}} + {}^{G,\text{new}}_{\text{wind}} * C_{\text{wind}} + {}^{G,\text{new}}_{\text{ess}} * C_{\text{ess}} + {}^{G,\text{new}}_{\text{pum}} * C_{pum} \end{array} \tag{3}$$

where $C^{\text{G}}_{\text{fix}}$ is fixed costs, $C^{\text{G}}_{\text{run}}$ is the sum of all power supply operating costs; $P^{G,\text{new}}_{\text{coal}}$, $P^{G,\text{new}}_{\text{hydro}}$, ${}^{G,\text{new}}_{\text{nuclear}}$, ${}^{G,\text{new}}_{\text{pv}}$, ${}^{G,\text{new}}_{\text{wind}}$, ${}^{G,\text{new}}_{\text{pum}}$, and ${}^{G,\text{new}}_{\text{ess}}$ are respectively the new installed capacities of thermal power, hydropower, nuclear power, photovoltaic power generation, wind power, pumped storage and energy storage; and C_{coal}, C_{hydro}, C_{nuclear}, C_{pv}, C_{wind}, C_{ess}, and C_{pum} are respectively the installed costs of a thermal power unit, hydropower unit, nuclear power unit, photovoltaic power unit, wind power unit, energy storage unit and pumped storage unit.

Due to the future expansion of renewable energy installations and the electricity demand from external regions, it is necessary to consider inter-regional grid transmission capacity in the planning process. The transmission channels between regions are simplified as capacity-type decision variables, with costs primarily including the investment in new transmission lines and the operational costs associated with regional interconnection and external power transfer. Accordingly, the external transmission cost of clean energy can be expressed as follows:

$$C^{\text{Trans}} = C^{\text{T}}_{\text{fix}} + C^{\text{T}}_{\text{run}} \tag{4}$$

where $C^{\text{T}}_{\text{fix}}$ is the sum of the investment cost of transmission line construction of transmission channel; $C^{\text{T}}_{\text{run}}$ is the sum of the operating costs of transmission lines in regional transmission channels.

(2) Objective 2: Maximization of Supply Reliability

The objective function also needs to consider supply reliability, which is measured using the load fluctuation rate as an indicator. The corresponding calculation formula is as follows:

$$\max f_2 = 1 - \frac{\left| \sum_i E^{\text{Gen}}_{a,i,y} - E_{\text{demand}} \right|}{E_{\text{demand}}} \tag{5}$$

where E_{demand} is the actual power demand, $E^{\text{Gen}}_{a,i,y}$ is the actual power generation of the power sources i, $\sum_i E^{\text{Gen}}_{a,i,y}$ is the actual power generation.

(3) Objective 3: Maximization of Renewable Energy Integration

During the operation period, renewable energy is preferentially dispatched to the grid whenever grid connection conditions are met.

$$\max f_3 = \sum_{t=1}^{T} (\mu_1 P_w(t) + \mu_2 P_{pv}(t)) / E^{\text{sum}}_{\text{new}} \tag{6}$$

where T is the length of running time, and μ_1 and μ_2 are the weighting factors for wind and PV; under normal circumstances, the two factors are equal. $P_w(t)$ denotes the wind power output at time t, $P_{pv}(t)$ denotes the photovoltaic output at time t, and $E^{\text{sum}}_{\text{new}}$ represents the total generation from wind and solar sources.

Constraints

(1) Power balance constraint

The sum of the total electricity demand and the output capacity of inter-regional transmission must not exceed the sum of the effective outputs of all generation units and the input capacity of inter-regional transmission.

$$L_a^{\max} + L * \sum_b P_{a,b}^{\text{Trans}} \leq L * [\sum_i (P_{a,i}^{G,\text{end}} \times \alpha_{a,i}) + \sum_b P_{b,a}^{\text{Trans}}] \tag{7}$$

where a denotes the local region, $L_a^{\max}$ represents the maximum electricity demand in region a, $P_{a,b}^{\text{Trans}}$ is the power transmitted from region a to region b, $P_{b,a}^{\text{Trans}}$ is the power transmitted from region b to region a, $\alpha_{a,i}$ is the reliability factor of the i-th type of generation unit in region a, $P_{a,i}^{G,\text{end}}$ denotes the installed capacity of the i-th type of generation unit in region a at the end of the year, and L is the transmission loss rate.

(2) Energy balance constraint

The sum of the generation from conventional power sources and the electricity imported from outside the province must equal the sum of the forecasted maximum electricity demand of the region and the electricity exported to external regions.

$$E_a^{\max l} + L * \sum_b E_{a,b}^{\text{Trans}} = L * (\sum_i E_{a,i}^{\text{Gen}} + \sum_b E_{\text{b,a}}^{\text{Trans}}) \tag{8}$$

where $E_a^{\max l}$ denotes the maximum electricity demand of region a; $E_{a,b}^{\text{Trans}}$ represents the electricity transmitted from region a to region b; $E_{a,i}^{\text{Gen}}$ is the electricity generated by the i-th type of generation unit in region a; and $E_{b,a}^{\text{Trans}}$ represents the electricity transmitted from region b to region a.

(3) Total installed capacity constraints

The annual installed capacity of conventional power sources should not exceed the policy target limits set for the region, while also satisfying the upper bounds imposed by the availability of wind, solar, and land resources.

$$P_{a,i,y-1}^{G,\text{end}} + P_{a,i}^{G,\text{new}} \leq P_{a,i}^{G,max} \tag{9}$$

where $P_{a,i,y-1}^{G,\text{end}}$ denotes the installed capacity of the i-th type of generation unit in region a at the end of the previous year; $P_{a,i}^{G,\text{new}}$ represents the newly added installed capacity of the i-th type of generation unit during the current year; and $P_{a,i}^{G,\max}$ denotes the maximum allowable installed capacity of the i-th type of generation unit at the end of the current year.

(4) Cross-regional transmission constraints

Cross-regional line construction should not exceed the limited capacity of the development and construction in this area.

$$P_{a,i,y-1}^{\text{Trans,end}} + P_{a,i}^{\text{Trans,new}} \leq P_{a,i}^{\text{Trans,max}} \tag{10}$$

where $P_{a,i,y-1}^{\text{Trans,end}}$ denotes the transmission capacity of the i-th type of transmission line at the end of the previous year; $P_{a,i}^{\text{Trans,new}}$ represents the newly installed capacity of the i-th type of transmission line during the current year; and $P_{a,i}^{\text{Trans,max}}$ denotes the maximum allowable deployment capacity of the i-th type of transmission line.

(5) Renewable energy penetration constraints

Since renewable energy is highly affected by natural conditions, its output is characterized by intermittency and volatility. In the process of building a new-type power system and facilitating the transformation of power grid enterprises, thermal power units are required to maintain the stable operation of the entire power system. Therefore, the development of renewable energy must proceed gradually; overly rapid expansion may result in excessively high penetration of renewables, thereby causing instability in the power system.

$$\sum_i (P_{a,i}^G \times H_{a,i}) \le K^{\max} \times E_a^{\mathrm{Gen}} \tag{11}$$

$$\sum_i (P_{a,i}^G \times H_{a,i}) \ge K^{\min} \times E_a^{\mathrm{Gen}} \tag{12}$$

where $P_{a,i}^G$ denotes the installed capacity of the i-th type of renewable energy unit in region a; $H_{a,i}$ represents the average utilization hours of the i-th type of renewable energy generation; $K^{\max}$ denotes the maximum allowable penetration rate of renewable energy; $K^{\min}$ denotes the minimum allowable penetration rate; and $E_{\mathrm{a}}^{\mathrm{Gen}}$ represents the electricity demand of region a.

(6) Carbon emission constraints

The annual emissions of coal-fired power plants and gas-fired power plants should not exceed certain limits.

$$\sum_i (E_{a,i}^{G,\mathrm{end}} \times I_{a,i}^C) \le R_a^{\mathrm{Max}} \tag{13}$$

where $E_{a,i}^{G,\mathrm{end}}$ denotes the electricity generation of the i-th type of generation unit in region a; $I_{a,i}^C$ represents the emission intensity of the i-th generation unit; and R_a^{Max} denotes the maximum allowable emissions i during year y.

(7) Peak-Shaving Reserve Constraint

Thermal power plants possess strong peak-shaving capabilities and play a critical role in deep peak regulation.

$$P_{a,1}^G \times D_{th} \ge P_W * W_a^{\max} + P_{pv} * PV_a^{\max} + P_{\mathrm{load}} * F_a^{\max} \tag{14}$$

where $P_{a,1}^G$ denotes the installed capacity of thermal power units in region a; D_{th} represents the depth of peak shaving for thermal units; P_{W} denotes the installed capacity of wind power; $W_a^{\max}$ represents the maximum fluctuation range of wind power output; P_{pv} denotes the installed capacity of PV; $PV_a^{\max}$ represents the maximum fluctuation range of PV power output; P_{load} denotes the maximum daily load; and $F_a^{\max}$ represents the maximum peak-to-valley ratio of the load.

2.1.2. Lower-Level Model for Sequential Production Cost Optimization

Objective Function

The optimization objective of the lower-level model is to minimize the total production cost of the new-type power system over an annual time horizon of 8760 h. The production cost includes the operation costs of generating units (e.g., hydropower, thermal power, nuclear power), start-up and shut-down costs, the penalty cost of renewable energy curtailment, and the penalty cost of load shedding. The optimization objective is expressed as follows:

$$f_1 = \min \sum_{t=1}^{\mathrm{T}} \begin{bmatrix} f_t^{\mathrm{coal}} + f_t^{\mathrm{nuclear}} + f_t^{\mathrm{hydro}} + f_t^{pum} + \\ f_t^{\mathrm{ess}} + \lambda_{\mathrm{RC}} P_t^{\mathrm{curW}} + \lambda_{\mathrm{LC}} P_t^{\mathrm{curL}} \end{bmatrix} \tag{15}$$

$$P_t^{\mathrm{curW}} = \left(P_{t\max}^{\mathrm{wind}} - P_t^{\mathrm{wind}}\right) + \left(P_{t\max}^{\mathrm{PV}} - P_t^{\mathrm{PV}}\right) \tag{16}$$

$$P_t^{\mathrm{curL}} = P_{\mathrm{load},t}^{\mathrm{pre}} - P_{\mathrm{load},t} \tag{17}$$

where f_t^{coal}, f_t^{hydro}, f_t^{nuclear}, f_t^{ess} and f_t^{pum} denote the generation cost of thermal power, hydropower, nuclear, battery storage, and pumped storage units at time t, respectively; λ_{RC} is the unit penalty cost of renewable energy curtailment; P_t^{curW} is the curtailed renewable energy at time t; λ_{LC} is the unit penalty cost of load shedding; and P_t^{curL} is the load shedding at time t. In addition, $P_{t\max}^{\mathrm{wind}}$ and P_t^{wind} represent the maximum available and actual output of wind power at time t, respectively; $P_{t\max}^{\mathrm{PV}}$ and P_t^{PV} represent the maximum available and actual output of photovoltaic power at time t, respectively; $P_{\mathrm{load},t}^{\mathrm{pre}}$ is the real-time system load; and $P_{\mathrm{load},t}$ is the portion of the load participating in system balancing at time t.

Constraints

(1) Power balance constraint

The new-type power system must always maintain a real-time balance between electricity supply and demand. The constraint is expressed as follows:

$$\begin{aligned}&\sum_{n=1}^{Npv} P_{\mathrm{pv}}(t,n) + \sum_{n=1}^{Nw} P_{\mathrm{w}}(t,n) + \sum_{n=1}^{Ncoal} P_{\mathrm{coal}}(t,n) + \sum_{n=1}^{Nnu} P_{\mathrm{nu}}(t,n) + \sum_{n=1}^{Nhydro} P_{\mathrm{h}}(t,n) + \sum_{n=1}^{Npum} P_{\mathrm{pum}}^{\mathrm{d}}(t,n) + \sum_{n=1}^{Ness} P_{\mathrm{ess}}^{\mathrm{d}}(t,n)\\ &+ \sum_{s=1}^{S} P_s(t,s) - P_t^{\mathrm{curW}} - \sum_{n=1}^{Npum} P_{\mathrm{pum}}^{c}(t,n) - \sum_{n=1}^{Ness} P_{\mathrm{ess}}^{\mathrm{c}}(t,n) - \sum_{n=1}^{Nnew} P_{\mathrm{new}}^{\mathrm{sum}}(t,n) = P_{\mathrm{load}}(t) - P_t^{\mathrm{curL}}\end{aligned} \tag{18}$$

where Npv, Nw, $Ncoal$, Nnu, $Nhydro$, $Npum$ and $Nnew$ denote the number of photovoltaic, wind, thermal, nuclear, hydro, pumped storage, battery storage, and total renewable units, respectively; $P_{\mathrm{coal}}(t,n)$, $P_{\mathrm{h}}(t,n)$ and $P_{\mathrm{nu}}(t,n)$ denote the output of the n-th thermal unit, hydro unit and nuclear unit, respectively; $P_{\mathrm{ess}}^{\mathrm{d}}(t,n)$ and $P_{\mathrm{pum}}^{\mathrm{d}}(t,n)$ denote the discharging power of battery storage and pumped storage at time t, respectively; $P_{\mathrm{ess}}^{\mathrm{c}}(t,n)$ and $P_{\mathrm{pum}}^{c}(t,n)$ denote the charging power of battery storage and pumped storage at time t, respectively; $P_{\mathrm{new}}^{\mathrm{sum}}$ denotes the curtailed renewable power, $P_{\mathrm{load}}(t)$ denotes the load demand, and $P_s(t,s)$ denotes the imported power of line S.

(2) Spinning Reserve Capacity Constraint

To ensure the security and reliability of the new-type power system, a certain level of spinning reserve capacity must be reserved. The spinning reserve is primarily provided by conventional thermal power units and hydropower units. The constraint is expressed as follows:

$$\begin{cases}\sum_{n=1}^{Ncoal}\left(P_{\mathrm{coal_max}}(n) - P_{\mathrm{coal}}(t,n)\right) + \sum_{n=1}^{Nhydro}\left(P_{\mathrm{hmax}}(n) - P_{\mathrm{h}}(t,n)\right) \geq S_{\mathrm{p}}\\ \sum_{n=1}^{Ncoal}\left(P_{\mathrm{coal}}(t,n) - P_{\mathrm{coal_min}}(n)\right) + \sum_{n=1}^{Nhydro}\left(P_{\mathrm{h}}(t,n) - P_{\mathrm{hmin}}(n)\right) \geq S_{\mathrm{N}}\end{cases} \tag{19}$$

where $P_{\mathrm{coal_max}}(n)$ and $P_{\mathrm{coal_min}}(n)$ denote the upper and lower output limits of the n-th thermal unit, respectively; $P_{\mathrm{hmax}}(n)$ and $P_{\mathrm{hmin}}(n)$ denote the upper and lower output limits of the n-th hydro unit, respectively; S_{p} and S_{N} represent the upward and downward spinning reserve requirements at time t, respectively.

The deterministic spinning reserve requirement is given by:

$$S_{\mathrm{P}} = S_{\mathrm{N}} \geq \left(P_{\mathrm{load}}(t) + \sum_{s=1}^{S} P_s(t,s)\right) \times w_{\mathrm{L}} + \left(P_w(t) + P_v(t)\right) \times w_W \tag{20}$$

where W_{L} is the load-based spinning reserve coefficient, $P_w(t)$ is the total wind power output at time t, $P_v(t)$ is the total photovoltaic power output, w_W is the spinning reserve coefficient associated with renewable energy variability.

(3) Ramp Rate Constraint for Thermal Units

The ramp rate constraint limits the maximum increase or decrease in output of thermal power units within a given time interval. The ramping capability of each unit is generally restricted by its physical characteristics. The constraint is expressed as:

$$\begin{cases} P_{\mathrm{f}}(t+1,n) - P_{\mathrm{f}}(t,n) \le P_{\mathrm{fup}}(n) \\ P_{\mathrm{f}}(t,n) - P_{\mathrm{f}}(t+1,n) \le P_{\mathrm{fdown}}(n) \end{cases} \tag{21}$$

where $P_{\mathrm{f}}(t,n)$ denotes the output of the n-th thermal unit at time t, $P_{\mathrm{f}}(t+1,n)$ denotes the output of the n-th thermal unit at time $t+1$, $P_{\mathrm{fup}}(n)$ and $P_{\mathrm{fdown}}(n)$ denote the maximum upward and downward ramp rates, respectively.

(4) Hydropower Unit Output Constraint

The output of hydropower units is limited by their minimum and maximum generation capacities. The constraint is expressed as:

$$P_{\mathrm{hmin}}(n) \le P_h(t,n) \le P_{\mathrm{hmax}}(n) \tag{22}$$

where $P_{\mathrm{hmin}}(n)$ and $P_{\mathrm{hmax}}(n)$ denote the minimum and maximum generation limits of the n-th hydropower unit, respectively.

(5) Nuclear Unit Output Constraint

The output of nuclear power units is constrained by their minimum and maximum generation limits to ensure safe operation of the nuclear plant. The constraint is expressed as:

$$P_{\mathrm{numin}}(n) \le P_{\mathrm{nu}}(t,n) \le P_{\mathrm{numax}}(n) \tag{23}$$

where $P_{\mathrm{numin}}(n)$ and $P_{\mathrm{numax}}(n)$ denote the minimum and maximum generation limits of the n-th nuclear unit, respectively.

(6) Charging and Discharging Constraints for Battery Storage and Pumped Storage

The charging and discharging power of storage systems cannot exceed their rated power. Moreover, the energy capacity of the storage system must remain within a specified range over a given period. For pumped storage plants, transitions between generation and pumping modes must pass through an idle state, which requires restricting the duration of the idle period. The constraints are expressed as follows:

$$\begin{cases} 0 \le P^{\mathrm{d}}_{\mathrm{ess}}(t,n) \le P^{\mathrm{d}}_{\mathrm{ess,max}}(t) \\ 0 \le P^{\mathrm{c}}_{\mathrm{ess}}(t,n) \le P^{\mathrm{c}}_{\mathrm{ess,max}}(t) \end{cases} \tag{24}$$

$$\begin{cases} 0 \le P^{\mathrm{d}}_{pum}(t,n) \le P^{\mathrm{d}}_{pum,\mathrm{max}}(t) \\ 0 \le P^{\mathrm{c}}_{pum}(t,n) \le P^{\mathrm{c}}_{pum,\mathrm{max}}(t) \end{cases} \tag{25}$$

where $P^{\mathrm{d}}_{\mathrm{ess,max}}(t)$ and $P^{\mathrm{d}}_{pum,\mathrm{max}}(t)$ denote the maximum discharging power of battery storage and pumped storage, respectively; $P^{\mathrm{c}}_{\mathrm{ess,max}}(t)$ and $P^{\mathrm{c}}_{pum,\mathrm{max}}$ denote the maximum charging power of battery storage and pumped storage, respectively.

(7) Transmission Channel Capacity Constraint

A regional power grid can both export and import electricity. The export/import power of interconnection lines is constrained as follows:

$$\begin{cases} P_{\mathrm{smin}}(s) \le P_s(t,s) \le P_{\mathrm{smax}}(s) \\ P_{\mathrm{SMIN}}(t) \le \sum\limits_{s=1}^{S} P_s(t,s) \le P_{\mathrm{SMAX}}(t) \end{cases} \tag{26}$$

where $P_{\mathrm{smin}}(s)$ and $P_{\mathrm{smax}}(s)$ denote the minimum and maximum of export and import power of line s; $P_{\mathrm{SMIN}}(t)$ and $P_{\mathrm{SMAX}}(t)$ denote the total planned maximum export and import power limits of the grid at time t.

(8) New energy output constraints

$$\begin{cases} 0 \le P_{\mathrm{w}}(t,n) \le P_{\mathrm{w}}^{*}(t) \\ 0 \le P_{\mathrm{pv}}(t,n) \le P_{\mathrm{pv}}^{*}(t) \end{cases} \tag{27}$$

where $P_{\mathrm{w}}^{*}(t)$ and $P_{\mathrm{pv}}^{*}(t)$ are respectively the predicted value of wind power and the PV power generation (theoretical output).

2.2. Capacity Configuration Decision Model Based on BWM–Entropy–TOPSIS

Based on the optimization model proposed in Section 2.1, it can be seen that the model presented in this paper includes multiple optimization objectives. Thus, it is necessary to evaluate these different objectives to select the optimal scheme. Although there are only three objectives, it is still essential to consider both subjective and subjective factors simultaneously and employ a suitable evaluation model to accurately assess the multiple schemes.

Therefore, to achieve a scientific and rational selection of power system capacity configuration schemes and overcome the subjectivity of traditional decision-making methods as well as the distortion of objective data, this study proposes an integrated decision-making model combining the BWM, Entropy Weight Method, and Technique for Order Preference by Similarity to Ideal Solution (TOPSIS).

Firstly, the BWM is applied to calculate the subjective weights of decision-makers, fully reflecting expert experience. Next, the Entropy Weight Method is used to compute objective weights based on the initial decision matrix of each scheme, effectively extracting information inherent in the data. The subjective and objective weights are then linearly combined to obtain comprehensive weights, balancing decision-maker preferences with data-inherent patterns. Finally, TOPSIS is employed to calculate the relative closeness of each configuration scheme to the positive and negative ideal solutions, enabling a complete ranking of all candidate schemes.

Assume that the capacity configuration decision problem involves m candidate configuration schemes A_b $(r = 1, 2, \ldots, m)$ and z evaluation criteria C_j $(j = 1, 2, \ldots, z)$, forming the initial decision matrix:

$$X = \begin{bmatrix} x_{11} & x_{12} & \cdots & x_{1z} \\ x_{21} & x_{22} & \cdots & x_{2z} \\ \vdots & \vdots & \ddots & \vdots \\ x_{m1} & x_{m2} & \cdots & x_{mz} \end{bmatrix} \tag{28}$$

2.2.1. Standardization of Decision Matrix

To eliminate differences in units and polarity (benefit-type or cost-type) among the evaluation criteria, the initial decision matrix X is normalized, resulting in a normalized matrix $R = (r_{bj})_{m \times z}$:

For benefit indicators:

$$r_{bj} = \frac{x_{bj} - \min_b(x_{bj})}{\max_b(x_{bj}) - \min_b(x_{bj})} \tag{29}$$

For cost indicators:

$$r_{bj} = \frac{\max_b(x_{bj}) - x_{bj}}{\max_b(x_{bj}) - \min_b(x_{bj})} \tag{30}$$

2.2.2. Determination of Combined Weights

Calculation of Subjective Weights Based on BWM

The BWM determines the most important (best) and least important (worst) criteria and compares them with all other criteria, greatly reducing the number of comparisons and improving consistency. The procedure is as follows:

Step 1. The decision-maker identifies the best criterion C_B and the worst criterion C_W from the set of evaluation criteria.

Step 2. Construct the Best-to-Others comparison vector: The decision-maker assigns importance values on a scale of 1–9 to express the relative importance of the best criterion with respect to all other criteria, forming the vector $A_B = (a_{B1}, a_{B2}, \ldots, a_{Bn})$, where a_{Bj} denotes the importance of criterion C_B relative to criterion C_j.

Step 3. Construct the Others-to-Worst comparison vector: The decision-maker assigns importance values on a scale of 1–9 to express the relative importance of all criteria with respect to the worst criterion, forming the vector $A_W = (a_{1W}, a_{2W}, \ldots, a_{nW})$.

Step 4. Formulate and solve an optimization model that minimizes the maximum absolute deviation to obtain the optimal subjective weights w_j^s .

$$\begin{aligned} &\min\max_j \left\{ \left| \frac{w_B^s}{w_j^s} - a_{Bj} \right|, \left| \frac{w_j^s}{w_W^s} - a_{jW} \right| \right\} \\ &\text{s.t.} \begin{cases} \sum_{j=1}^{n} w_j^s = 1 \\ w_j^s \geq 0,\ j = 1, 2, \cdots, n \end{cases} \end{aligned} \tag{31}$$

Calculation of Objective Weights Based on the Entropy Method

The Entropy Weight Method determines the weights of evaluation criteria based on the degree of variation in their values. A smaller information entropy indicates greater variability of the criterion, and thus a higher weight. The procedure is as follows:

Step 1. Compute the proportion p_{bj} of the b-th scheme under the j-th criterion:

$$p_{bj} = \frac{r_{bj}}{\sum_{b=1}^{m} r_{bj}} \tag{32}$$

Step 2. Calculate the entropy e_j of the j-th criterion:

$$e_j = -k \sum_{b=1}^{m} p_{bj} \ln(p_{bj}),\ \text{where } k = 1/\ln(m) \tag{33}$$

Step 3. Compute the differentiation coefficient g_j of the j-th criterion:

$$g_j = 1 - e_j \tag{34}$$

Step 4. Calculate objective weights w_j^o:

$$w_j^o = \frac{g_j}{\sum_{j=1}^{n} g_j} \tag{35}$$

Calculation of Combined Weights

The subjective and objective weights are integrated using a linear weighting method to obtain the comprehensive weight w_j^c.

$$w_j^c = \alpha w_j^s + (1-\alpha) w_j^o \tag{36}$$

where $\alpha \in [0,1]$ is the preference coefficient, which can be adjusted according to the decision-maker's preference between subjective experience and objective data. When $\alpha = 0.5$, subjective and objective weights are considered equally important.

2.2.3. Scheme Ranking Based on TOPSIS

The TOPSIS model ranks the candidate schemes by calculating their relative closeness to the ideal solution. The procedure is as follows:

Step 1. Construct the weighted normalized decision matrix V:

$$V = (v_{bj})_{m\times z} = (w_j^c \cdot r_{bj})_{m\times z} \tag{37}$$

Step 2. Determine the positive ideal solution V^+ and negative ideal solution V^-:

$$\begin{cases} V^+ = (v_1^+, v_2^+, \ldots, v_n^+) = \left(\max_i v_{bj} \,\middle|\, j \in J\right) \\ V^- = (v_1^-, v_2^-, \ldots, v_n^-) = \left(\min_i v_{bj} \,\middle|\, j \in J\right) \end{cases} \tag{38}$$

where J represents the set of indicators.

Step 3. Calculate the Euclidean distance of each scheme to the positive and negative ideal solutions:

$$\begin{cases} D_b^+ = \sqrt{\sum_{j=1}^{n} (v_{bj} - v_j^+)^2} \\ D_b^- = \sqrt{\sum_{j=1}^{n} (v_{bj} - v_j^-)^2} \end{cases} \tag{39}$$

Step 4. Compute the relative closeness C_i of each scheme to the positive ideal solution:

$$C_b = \frac{D_i^-}{D_i^+ + D_i^-},\ 0 \le C_i \le 1 \tag{40}$$

Step 5. Rank the candidate schemes in descending order of C_i . A higher C_i indicates a better scheme.

2.3. NSGA-II Algorithm

The NSGA-II algorithm significantly improves the convergence speed and precision of optimization, making it one of the most widely used multi-objective optimization algorithms. It holds a significant position in multi-objective optimization for fields such as energy, electric power, and chemical engineering. Since this study considers multiple objectives, including cost minimization and power supply reliability, it is necessary to find the Pareto-optimal solution set. The NSGA-II algorithm directly identifies the Pareto-optimal solution set through non-dominated sorting; therefore, it was selected in this paper to solve the optimization model. Figure 1 shows the flowchart of the NSGA-II algorithm.

2.4. Research Framework

This study establishes a two-stage decision-making framework for power system capacity optimization, where the upper-level problem focuses on capacity expansion planning and the lower-level problem addresses chronological production simulation and operational optimization. A bi-level robust capacity optimization model considering multiple objectives is constructed, and a capacity configuration scheme decision-making

method based on the BWM–Entropy–TOPSIS model is integrated. The decision-making process is illustrated in Figure 2 and described as follows:

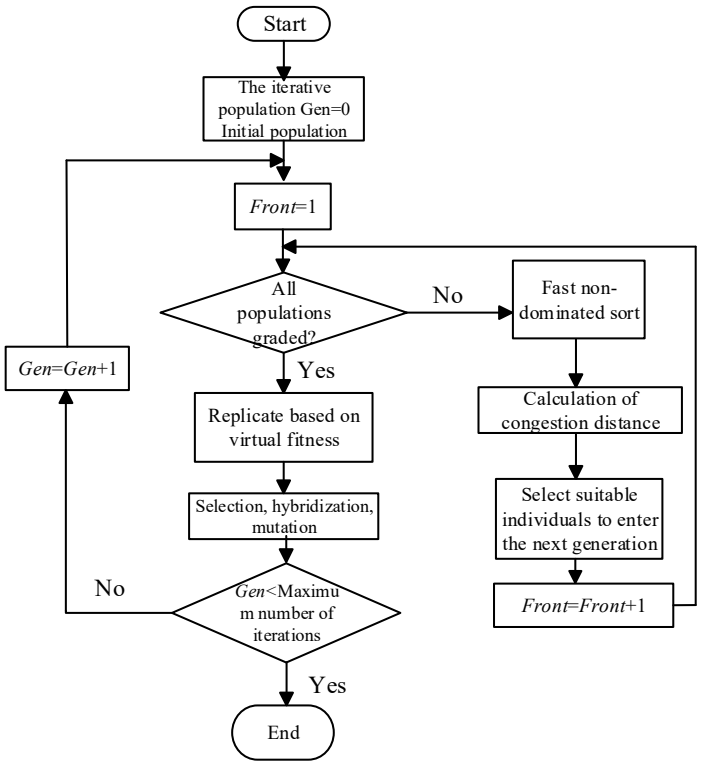


Figure 1. Flowchart of the NSGA-II algorithm.

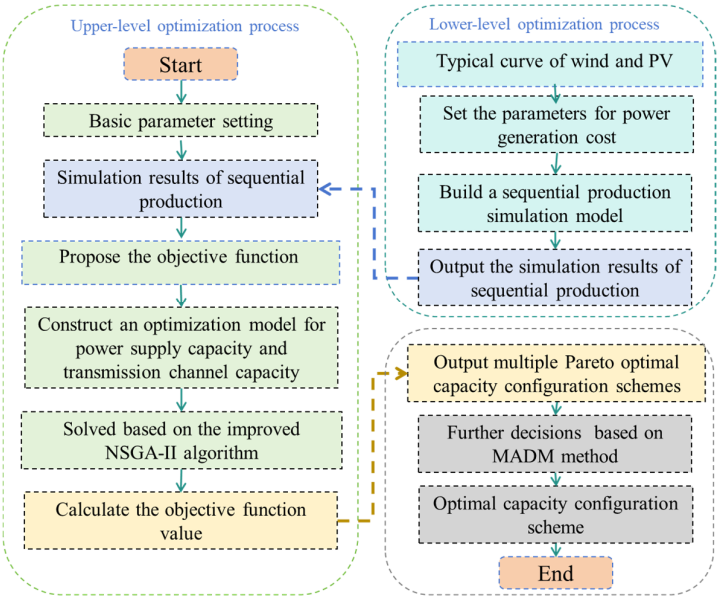


Figure 2. Two-stage capacity optimization configuration decision framework.

Step 1. Generate multiple scenarios, including extreme weather conditions, based on historical data;

Step 2. Construct the upper-level multi-objective capacity optimization model, with objectives including minimizing investment costs for generation and transmission capacity, maximizing renewable energy integration, and maximizing supply reliability;

Step 3. Construct the lower-level chronological production optimization model with the objective of minimizing operational costs;

Step 4. Integrate the upper- and lower-level objectives to form the bi-level optimization model and obtain multiple capacity configuration schemes on the Pareto frontier;

Step 5. Evaluate the multiple capacity configuration schemes using the BWM–Entropy–TOPSIS method to select the multi-objective optimal configuration scheme.

3. Case Study

3.1. Basic Parameter Settings

This paper selects a region in Shandong Province of China for case study analysis. The power system in this region contains various types of power sources including hydropower, wind power, photovoltaic, nuclear power, thermal power, energy storage, and pumped storage. Meanwhile, as an energy demand side, this region needs to obtain external electricity through transmission channels. The system structure is shown in Figure 3 and Table 1. In this case study, the operation of a high-renewable-penetration power system over a one-year period (8760 h) is considered, with hourly generation and load data for all types of power sources.

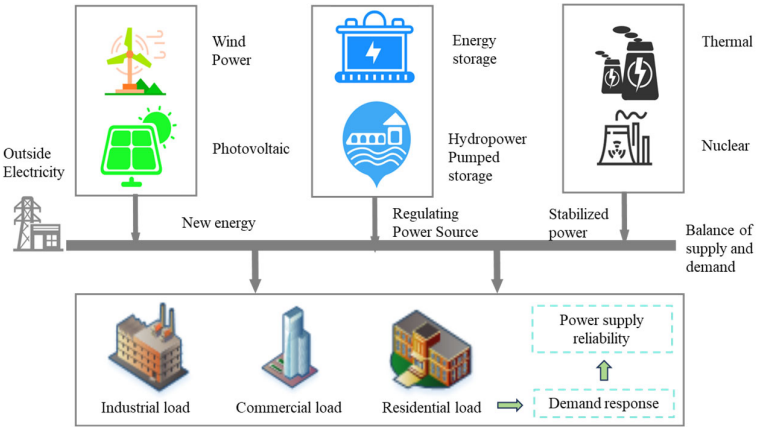


Figure 3. Schematic diagram of the power system.

Table 1. System Operating Parameters.

Types	Regional Installed Capacity/MW	Reliability Factor	Maximum Installed Capacity Constraint/MW	Maximum Added Value	Utilization Hours	Maximum Penetration Rate
Photovoltaic	7610	0.3	8610	1000	1100	0.3
Wind	2670	0.3	3670	1000	1900	0.9
Thermal	12,120	0.78	12,620	500	4300	0.2
Nuclear	418	0.92	418	0	7600	0.6
Hydropower	7	0.85	27	20	1500	0.3
Pumped storage	400	/	800	400	1500	/
Energy storage	800	0.2	1100	300	/	/

Based on references [26–28], the installed costs and operational costs for various power sources such as wind and photovoltaic power are compiled and presented in Table 2.

To reflect practical considerations, the installed capacities of wind, solar, and storage units are all treated as integer values. The incremental capacities are set as follows: 20 MW for wind power, 10 MW for photovoltaic (PV) units, 20 MW for thermal power, 40 MW/100 MWh for pumped storage (allowing full-power pumping for 10 h), and 10 MW/2 MWh for energy storage systems (allowing full-power charging for 2 h). Both wind and solar curtailment factors are set to 1, and the transmission loss rate is assumed to be 4%.

Table 2. Investment Cost Parameters of Various Types of power supplies.

Types	Installation Cost (Ten Thousand Yuan/MW)	Annual Maintenance Cost (Ten Thousand Yuan/MW·Year)
Photovoltaic	380	3
Wind	600	6
Thermal	400	15
Nuclear	1500	25
Hydropower	840	6
Pumped storage	800	10
Energy storage	150	10
Transmission line cost	1300	15

3.2. Capacity Optimization Configuration Schemes

(1) Pareto-optimal Capacity Configuration Results

Taking a 30-day chronological production simulation of the new-type power system as an example, multiple capacity configuration schemes were obtained after 100 generations, as shown in Figure 4. Among the 20 candidate schemes, the top 10 are identified as Pareto-optimal solutions. It can be observed that, within the Pareto set, the additional installed capacities of photovoltaic (PV) units and transmission lines are consistent, whereas significant differences exist in wind power and energy storage capacities, with relatively minor differences in thermal power capacities. Regarding the objective functions, the range of *F1* (investment and operational costs) is 1,430,000–1,450,000, the range of *F2* (supply reliability) is 0.997–0.999, and the range of *F3* (renewable energy integration) is 0.97–0.99. Since all 10 solutions belong to the Pareto frontier, further decision-making is required to select the most suitable capacity configuration scheme.

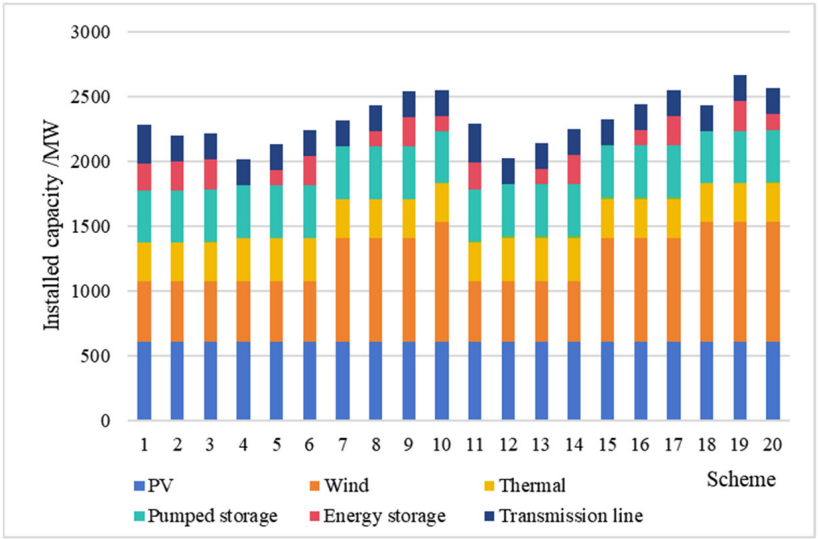


Figure 4. Capacity Optimization Scheme.

3.3. Selection of Capacity Configuration Scheme Based on Multi-Attribute Decision Making

First, the weights of the three objectives were calculated using the BWM and the entropy weighting method, respectively, and then combined to obtain comprehensive weights. The results are presented in Table 3. It can be observed that there are considerable differences between subjective and objective weighting, and the use of integrated weighting is more reasonable. According to the subjective weighting results, experts considered the system's annual investment cost as the most important objective with a weight of 0.3867, followed by supply reliability, and finally renewable energy integration.

Table 3. Results of multi-objective weighting.

Method	*F1*	*F2*	*F3*	Method Weight
BWM	0.3867	0.3272	0.2861	0.4
Entropy weight	0.3417	0.2733	0.3850	0.6
Combination weighting	0.3597	0.2949	0.3454	/

Subsequently, a sensitivity analysis was conducted on the weights of different indicators. Scenario 1 serves as the baseline scenario, where objective *F1* has the highest weight; Scenario 2 and 3 represent the cases where objective *F2* and objective *F3* have the highest weights, respectively.

The ten candidate schemes were then evaluated and compared using the TOPSIS model, and the final evaluation results are shown in Figure 5. From the ranking results, scheme S1 achieved the highest score, whereas schemes S7 and S10 scored lower. Therefore, scheme S1 is recommended as the optimal capacity configuration.

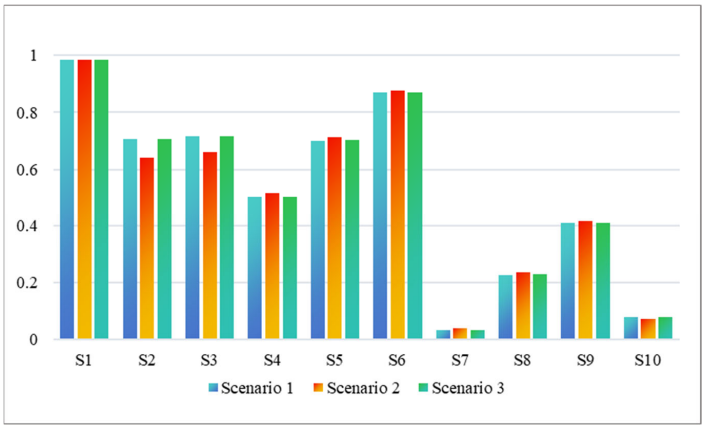


Figure 5. Evaluation results of the schemes.

Table 4 presents the optimal and inferior solutions under the three scenarios. According to Figure 5 and Table 4, as the indicator weights change, the optimal solution remains S1, and the inferior solution remains S7. Furthermore, the evaluation results and rankings of other solutions show minimal variation. This demonstrates that solution S1 remains the optimal choice despite changes in objective weights, indirectly validating the effectiveness of the proposed capacity configuration optimization model in this study.

Table 4. Evaluation Results under different index weights.

Method	*F1*	*F2*	*F3*	Optimal Scheme	Worst Scheme
Scenario 1	0.3597	0.2949	0.3454	S1	S7
Scenario 2	0.2949	0.3597	0.3454	S1	S7
Scenario 3	0.3454	0.2949	0.3597	S1	S7

3.4. Power Balance Analysis Under the Optimal Scheme

Under the optimal configuration scheme S1, the capacity expansion results are as follows: additional installed capacities of 610 MW for photovoltaic (PV) units, 460 MW for wind power, 300 MW for thermal power, 400 MW for pumped storage, 210 MW for energy storage, and 300 MW for transmission lines.

The optimized hourly outputs of each type of generation over 720 h under scheme S1 are shown in Figure 6. Based on these multi-type generation outputs and the corresponding load data, a detailed power balance analysis can be conducted. It can be observed that the

output of thermal power and renewable energy sources such as wind and solar exhibits a complementary relationship, demonstrating the safeguarding and regulating capabilities of thermal power.

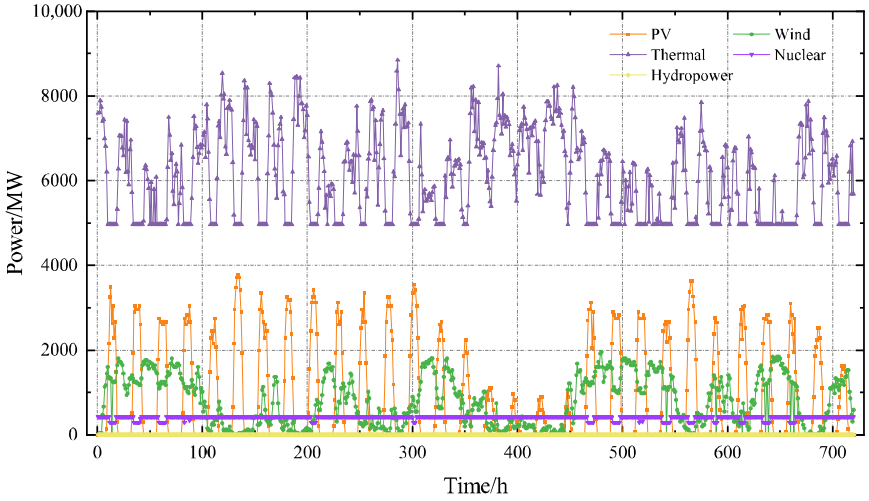


Figure 6. The power generation capacity of different power sources under S1.

Under scheme S1, the charging and discharging profiles of pumped storage and energy storage systems are shown in Figure 7. It can be seen that the utilization rates of energy storage and pumped storage are relatively low during periods of low wind and solar output, while they are significantly higher during peak solar power generation hours (11:00–15:00). This highlights the critical role of energy storage and pumped storage in maintaining power and energy balance.

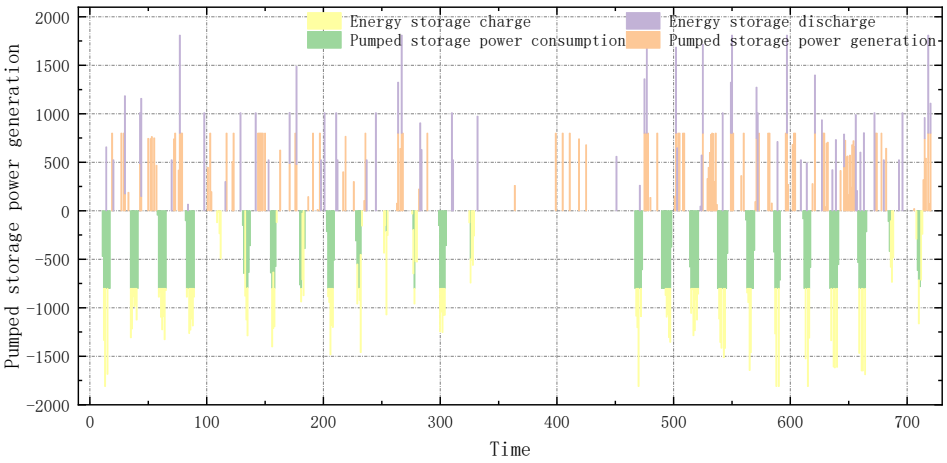


Figure 7. The energy storage charge and discharge capacity under S1.

The curtailed renewable energy is shown in Figure 8. It can be observed that under scheme S1, the amount of curtailed renewable energy is relatively low, with a renewable energy utilization rate of 98.5%. The results prove the effectiveness of the proposed method in achieving the integration and utilization of renewable energy.

The power generation and consumption, as well as the transmission line load, are illustrated in Figure 9. It can be seen that under scheme S1, a power supply reliability of 99.8% is ensured, essentially achieving a balance between power supply and demand.

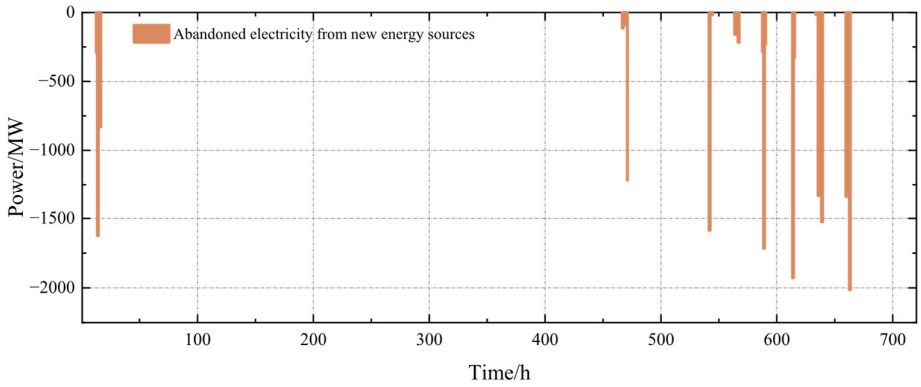


Figure 8. The abandoned electricity of new energy under S1.

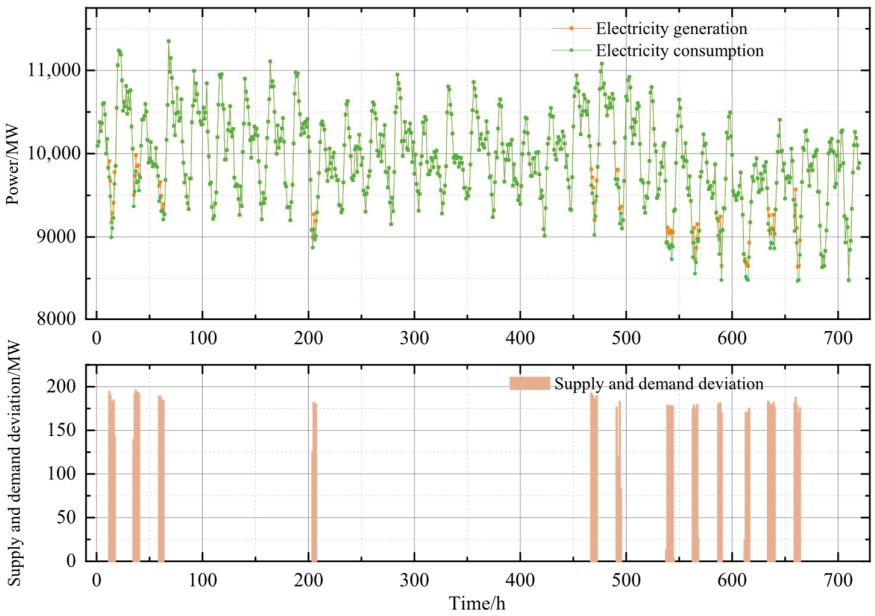


Figure 9. The power supply and demand balance curve under S1.

3.5. Multi-Scenario Analysis

To demonstrate the advantages of the method proposed in this paper, the calculation results are compared and analyzed against the results from a single-objective optimization (Scenario M1), as well as the results obtained using the multi-objective particle swarm optimization algorithm (Scenario M2) and the multi-objective grey wolf optimizer algorithm (Scenario M3). Scenario 1 serves as the baseline scenario, which considers the minimization of investment cost as the objective, determining the optimal capacity configuration that meets the normal operation requirements of the power system. Scenarios 2 and 3 represent the results obtained by applying different optimization algorithms to solve the model proposed in this paper. The results calculated using these different optimization algorithms are presented in Table 5.

Table 5. Comparison of results under different algorithms.

	Algorithm	***F1***	***F2***	***F3***
Optimal scheme under M1	Single-objective optimization	1,426,247.03	0.9979	0.9794
Optimal scheme under M2	MOPSO	1,440,217.67	0.9980	0.9850
Optimal scheme under M3	MOGWO	1,441,459.77	0.9983	0.9816
Optimal scheme under M4	NSGA-II	1,440,374.16	0.9985	0.9850

The results indicate that the single-objective optimization model achieves the lowest investment cost but struggles to guarantee power supply reliability and the new energy utilization rate. Specifically, compared to the single-objective optimization algorithm, the NSGA-II algorithm improves power supply reliability by 0.06% and increases the new energy utilization rate by 0.56%. Furthermore, while the MOPSO and MOGWO algorithms demonstrate higher optimization efficiency, the optimization results obtained using the NSGA-II algorithm yield better outcomes in terms of both power supply reliability and new energy utilization. Thus, overall, NSGA-II is more suitable for multi-objective capacity configuration optimization in power systems.

Furthermore, to assess the robustness of the proposed decision-making framework under various scenarios, including extreme weather conditions, this section further analyzes the results of the power system capacity optimization considering the uncertainty of wind and solar outputs. Nine scenarios shown in Table 6 are considered in which wind and solar outputs are reduced continuously for one week. Among them, scenario M12 represents an extreme weather event in which wind and solar outputs randomly decrease by 30% for a full week.

Table 6. Multi-scenario settings of uncertainty in wind and solar power output.

Scenario	M4	M5	M6	M7	M8	M9	M10	M11	M12
Wind power	0%	0%	0%	−5%	−5%	−5%	0%	−20%	−30%
PV power	0%	−5%	−10%	0%	−5%	10%	0%	−10%	−30%

Using the same capacity optimization decision-making framework, the optimal capacity configuration scheme is selected, and the corresponding objective values of investment and operational costs (*F1*), supply reliability (*F2*), and renewable energy integration (*F3*) are calculated for each scenario, as shown in Figure 10.

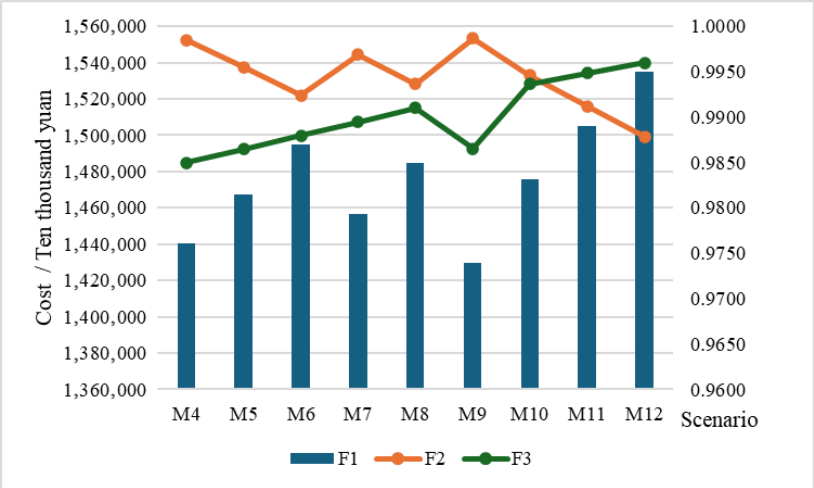


Figure 10. Multi-objective calculation results in multiple scenarios.

It can be observed that as wind and solar outputs decrease, supply reliability gradually declines, while renewable energy integration gradually increases. However, even under the extreme weather scenario, supply reliability remains above 98.78%, and renewable energy integration exceeds 98.50%. These results demonstrate that the proposed two-stage capacity optimization and configuration decision-making framework exhibits strong effectiveness and robustness, providing valuable guidance for power balance management and mid- to long-term power system planning.

4. Conclusions and Limitations

4.1. Conclusions

This study proposes a mid–long-term regional capacity optimization model based on chronological production simulation. Firstly, by employing a bi-level dynamic iterative mechanism, mid- to long-term capacity planning is deeply coupled with short-term operational simulation, addressing the disconnection between planning schemes and actual operational requirements inherent in traditional hierarchical optimization, and achieving a globally optimal balance between investment and operational costs. Secondly, the model embeds objectives to maximize renewable energy integration, thereby promoting efficient resource allocation and enhanced curtailment mitigation between renewable-rich areas and load centers. The main conclusions are as follows:

(1) The proposed bi-level power system capacity optimization model in this paper considers economic–social–environmental multi-objectives, maintaining low costs while ensuring a 99.8% power supply reliability and a 98.5% new energy utilization rate.

(2) The BWM–Entropy–TOPSIS-based capacity configuration scheme decision-making model effectively identifies the multi-objective optimal configuration scheme.

(3) Under the proposed two-stage robust power system capacity configuration optimization decision-making framework, the model can effectively handle complex scenarios such as extreme weather, maintaining 98.7% power supply reliability even under such conditions and further increasing the new energy utilization rate.

In summary, the proposed two-stage robust capacity optimization framework for power systems, which incorporates multiple objectives, simultaneously considers power balance and mid- to long-term planning optimization, demonstrating good stability and effectiveness in practical applications.

4.2. Research Limitations and Prospects

Nevertheless, some limitations remain in this study. Firstly, the model does not account for uncertainties in energy prices, the evolution of future carbon policies, or the potential impacts of emerging technologies, which may affect the long-term robustness of the research findings. Secondly, although the proposed optimization method is effective, its high computational burden may restrict its application to larger-scale systems. Thirdly, the case study is confined to a specific region, limiting the generalizability of the conclusions. Finally, the current multi-attribute decision-making process does not account for differences in expert opinions.

Future research could be deepened in the following directions: Firstly, introducing methods such as stochastic programming or robust optimization to incorporate uncertainties in key parameters like energy prices and carbon taxes, thereby enhancing the robustness of decision-making. Secondly, exploring more efficient computational algorithms or parallel computing techniques to improve the model's capability to solve large-scale practical problems. Thirdly, applying the research framework to case studies in different regions or countries for comparative validation, in order to test and enhance its generalizability. Fourthly, introducing group decision-making methods that consider expert weights or handle opinion conflicts in the decision-making process, making the decision results more aligned with practical realities.

Author Contributions: Z.W.: writing—original draft, X.J.: writing—review and editing; Z.F.: writing—original draft preparation; Y.W.: writing—original draft preparation. All authors have read and agreed to the published version of the manuscript.

Funding: This research is supported by the Science and Technology Project of the Headquarters of State Grid Corporation of China (Research on Medium and Long-Term Electric Power and Energy

Balance Method for New Power System Considering Multiple Uncertainties, No. 5100-202358689A-3-3-JC).

Data Availability Statement: Data is contained within the article.

Conflicts of Interest: The authors declare no conflicts of interest.

Abbreviations

The following abbreviations are used in this manuscript:

i	power sources
a	the regional power system of this study
y	the years when investment in various types of power supplies is required
t	time
C^{Gen}	power installation cost
C^{Trans}	construction cost of the power transmission lines
$C^{\mathrm{G}}_{\mathrm{fix}}$	fixed costs
$C^{\mathrm{G}}_{\mathrm{run}}$	power supply operating costs
$C^{\mathrm{T}}_{\mathrm{fix}}$	sum of the investment cost of transmission line
$C^{\mathrm{T}}_{\mathrm{run}}$	sum of the operating costs of transmission lines
E_{demand}	actual power demand
$E^{\mathrm{Gen}}_{a,i,y}$	actual power generation of the power sources i
$L^{\max}_{a}$	maximum electricity demand in region a
$P^{\mathrm{Trans}}_{a,b}$	the power transmitted from region a to region b
$E^{\max l}_{a}$	the maximum electricity demand of region a
$P^{\mathrm{G,end}}_{a,i,y-1}$	the installed capacity of the i-th type of generation unit in region a at the end of the previous year
$P^{\mathrm{Trans,end}}_{a,i,y-1}$	transmission capacity of the i-th type of transmission line at the end of the previous year
$P^{G}_{a,i}$	the installed capacity of the i-th type of renewable energy unit in region a
$E^{\mathrm{G,end}}_{a,i}$	the electricity generation of the i-th type of generation unit in region a
f^{coal}_{t}	generation cost of thermal power
P^{curW}_{t}	the curtailed renewable energy at time t
Npv	the number of photovoltaic units
$P_{\mathrm{coal}}(t,n)$	output of the n-th thermal unit
$P_{\mathrm{load}}(t)$	load demand of time t
$P_{s}(t,s)$	the imported power of line S
$P_{\mathrm{coal_max}}(n)$	upper output limits of the n-th thermal unit
$P_{\mathrm{f}}(t,n)$	output of the n-th thermal unit at time t
$P^{\mathrm{d}}_{\mathrm{ess,max}}(t)$	the maximum discharging power of battery storage
b	the investment scheme for capacity configuration of power systems
j	evaluation criteria
m	the total number of schemes
z	the total number of criteria
C_B	the best criterion
C_W	the worst criterion
w^{s}_{j}	optimal subjective weights
w^{o}_{j}	objective weights
w^{c}_{j}	the comprehensive weight
C_b	the relative closeness of each scheme to the positive ideal solution

References

1. Zhao, H.; Yuan, S.; Peng, D.; Li, T. A two-stage optimization operation method for low-carbon demand response in molten salt manufacturing process considering dynamic carbon potential and price signals of grid electricity. *Renew. Energy* **2026**, *256*, 123900. [CrossRef]
2. Li, G.; Luo, Z.; Liao, C. Power capacity optimization and long-term planning for a multi-energy complementary base towards carbon neutrality. *Energy* **2025**, *334*, 137644. [CrossRef]
3. Pan, T.; Zhao, Q.; Zhao, J.; Wang, L. Research on the Low-Carbon Economic Operation Optimization of Virtual Power Plant Clusters Considering the Interaction Between Electricity and Carbon. *Processes* **2025**, *13*, 1943. [CrossRef]
4. Porcelli, R.; Gibon, T.; Marazza, D.; Righi, S.; Rugani, B. Prospective environmental impact assessment and simulation applied to an emerging biowaste-based energy technology in Europe. *Renew. Sustain. Energy Rev.* **2023**, *176*, 113172. [CrossRef]
5. Movsessian, M.M.; Oyewo, A.S.; Aghahosseini, A.; Breyer, C. Enabling Central America's energy transition through renewable energy, energy citizenship, and regional integration. *Appl. Energy* **2025**, *377*, 124493. [CrossRef]
6. Ali, M.A.; Bhatti, A.R.; Rasool, A.; Farhan, M.; Esenogho, E. Optimal Location and Sizing of Photovoltaic-Based Distributed Generations to Improve the Efficiency and Symmetry of a Distribution Network by Handling Random Constraints of Particle Swarm Optimization Algorithm. *Symmetry* **2023**, *15*, 1752. [CrossRef]
7. Yuan, J.; Zhang, K.; Ding, B.; Huangfu, W.; Zhang, J.; Mou, Q.; Peng, K.; Zhang, H. Enhancement strategy of power system resilience for supply-demand imbalance at extreme weather conditions: A high-share renewable energy case from Qinghai Province in China. *Renew. Energy* **2026**, *256*, 124048. [CrossRef]
8. Li, X.; Li, Y.; Tan, Q.; Zhang, S. Bi-objective robust dispatch model for virtual power plant with security-economy-green equilibrium in the new-type power system. *Energy Convers. Manag.* **2025**, *344*, 120253. [CrossRef]
9. Koch, C.; Hirth, L. Short-term electricity trading for system balancing: An empirical analysis of the role of intraday trading in balancing Germany's electricity system. *Renew. Sustain. Energy Rev.* **2019**, *113*, 109275. [CrossRef]
10. Yalili, M.; Menlik, T.; Boran, F.E. A novel multi-objective decision-making model to determine optimum resource and capacity configuration for hybrid electricity generation systems: A comparative case study in Turkiye. *Appl. Energy* **2024**, *376*, 124338. [CrossRef]
11. Zhang, S.; Xiang, Y.; Liu, J.; Liu, J.; Yang, J.; Zhao, X.; Jawad, S.; Wang, J. A regulating capacity determination method for pumped storage hydropower to restrain PV generation fluctuations. *CSEE J. Power Energy Syst.* **2022**, *8*, 304–316.
12. Jiang, H.; Du, E.; Zhang, N.; Zhuo, Z.; Wang, P.; Wang, Z.; Zhang, Y. Renewable Electric Energy System Planning Considering Seasonal Electricity Imbalance Risk. *IEEE Trans. Power Syst.* **2023**, *38*, 5432–5444. [CrossRef]
13. Cepeda, J.C.; Echeverria, D.E.; Chamba, M.S.; Kamwa, I.; Rueda-Torres, J.L. Wide-Area Monitoring Protection and Control Supported Operation and Planning in the Ecuadorian Power System: Improving Security and Reliability. *IEEE Power Energy Mag.* **2025**, *23*, 59–68. [CrossRef]
14. Tangi, M.; Amaranto, A. Designing integrated and resilient multi-energy systems via multi-objective optimization and scenario analysis. *Appl. Energy* **2025**, *382*, 125281. [CrossRef]
15. Lei, Z.; Yu, H.; Li, P.; Ji, H.; Yan, J.; Song, G.; Wang, C. A compact time horizon compression method for planning community integrated energy systems with long-term energy storage. *Appl. Energy* **2024**, *361*, 122912. [CrossRef]
16. Fu, X.; Zhang, C.; Zhang, X.; Sun, H. A Novel GAN Architecture Reconstructed Using Bi-LSTM and Style Transfer for PV Temporal Dynamics Simulation. *IEEE Trans. Sustain. Energy* **2024**, *15*, 2826–2829. [CrossRef]
17. Cheng, Y.; Zhang, N.; Kirschen, D.S.; Huang, W.; Kang, C. Planning multiple energy systems for low-carbon districts with high penetration of renewable energy: An empirical study in China. *Appl. Energy* **2020**, *261*, 114390. [CrossRef]
18. Zhang, H.; Liao, K.; Yang, J.; Zheng, S.; He, Z. Frequency-constrained expansion planning for wind and photovoltaic power in wind-photovoltaic-hydro-thermal multi-power system. *Appl. Energy* **2024**, *356*, 122401. [CrossRef]
19. Verastegui, F.; Lorca, A.; Olivares, D.E.; Negrete-Pincetic, M.; Gazmuri, P. An Adaptive Robust Optimization Model for Power Systems Planning with Operational Uncertainty. *IEEE Trans. Power Syst.* **2019**, *34*, 4606–4616. [CrossRef]
20. Nunes, J.B.; Mahmoudi, N.; Saha, T.K.; Chattopadhyay, D. A multi-stage transition toward high renewable energy penetration in Queensland, Australia. *IET Gener. Transm. Distrib.* **2018**, *12*, 850–858. [CrossRef]
21. Li, D.; Liu, H.; Zhang, J.; Han, X.; Zhang, S. Multistage power generation planning approach for new power systems with high renewable energy integration considering flexibility constraints. *Int. J. Electr. Power Energy Syst.* **2025**, *169*, 110818. [CrossRef]
22. Suo, X.; Zhao, S.; Ma, Y. Multipoint layout planning method for multi-energy sources based on time-series production simulation. *Int. J. Energy Res.* **2022**, *46*, 9323–9344. [CrossRef]
23. Li, H.; Lu, Z.; Qiao, Y.; Wang, N. A Non-Sequential Probabilistic Production Simulation Method for Wind Energy Curtailment Evaluation Considering the Seasonal Heat Supply Constraints. *IEEE Trans. Sustain. Energy* **2018**, *9*, 462–473. [CrossRef]
24. Qi, Z.; Guo, S.; Zhao, H. Research on quantitative evaluation and optimal allocation of electricity system flexibility. *Energy* **2025**, *320*, 135443. [CrossRef]

25. Yang, Y.; Lu, Q.; Yu, Z.; Wang, W.; Hu, Q. Multi-Type Energy Storage Collaborative Planning in Power System Based on Stochastic Optimization Method. *Processes* **2024**, *12*, 2079. [CrossRef]
26. Zhang, M.; Cong, N.; Song, Y.; Xia, Q. Cost analysis of onshore wind power in China based on learning curve. *Energy* **2024**, *291*, 130459. [CrossRef]
27. Elfeky, K.E.; Wang, Q. Techno-environ-economic assessment of photovoltaic and CSP with storage systems in China and Egypt under various climatic conditions. *Renew. Energy* **2023**, *215*, 118930. [CrossRef]
28. Huang, D.; Chen, B.; Yu, N.; Yang, D.; Kong, L. Comprehensive Energy Station Equipment Selection and Capacity Optimization Allocation Based on Vertex Graph Decomposition and Merging Principle. In Proceedings of the CSEE 2025, Nanjing, China, 21–23 February 2025; pp. 453031–453046.

Disclaimer/Publisher's Note: The statements, opinions and data contained in all publications are solely those of the individual author(s) and contributor(s) and not of MDPI and/or the editor(s). MDPI and/or the editor(s) disclaim responsibility for any injury to people or property resulting from any ideas, methods, instructions or products referred to in the content.